Journal of *Marine Science and Engineering*

MDPI

Article

Coupled Source-to-Sink Relationships in a Rifted Lacustrine Basin: A Case Study of the Eocene Wenchang Formation Member 6 (W6), Yangjiang East Sag, Pearl River Mouth Basin

Shangfeng Zhang [1,2,*], Linyuan Shi [1], Yaning Wang [1,2], Gaoyang Gong [1], Rui Han [1] and Xinwei Qiu [3]

[1] School of GeoSciences, Yangtze University, Wuhan 430100, China; linyshi@163.com (L.S.)
[2] Key Laboratory of Exploration Technologies for Oil and Resources, Ministry of Education, Yangtze University, Wuhan 430100, China
[3] Shenzhen Branch, CNOOC China Limited, Shenzhen 518000, China
* Correspondence: jpuzhangsf@163.com

Abstract

The formation and spatial distribution of sedimentary systems in rift-lake basins are jointly controlled by multiple factors, including sediment supply rates from source areas, clastic sediment transport pathways, and basin geometry and intrabasinal structural configuration (e.g., accommodation zones and faults), which strongly influence the architecture of depositional systems and basin filling processes. The Wenliu Formation (Wenliu Member, Late Paleogene) of the Wenchang Group in the Enping 20/21 Depression of the Yangjiang East Sag, Pearl River Mouth Basin, developed a multi-source and multi-channel sand-transport system; however, the matching relationships and coupling mechanisms among different source areas, transport pathways, and depositional systems remain poorly understood. Based on three-dimensional seismic data, drilling, and well-log information, combined with heavy mineral assemblages and detrital zircon U–Pb age spectra, this study comprehensively investigates the source areas, paleochannel clastic sediment transport pathways, and depositional systems of the Wenliu Member, systematically establishing the source-to-sink (S2S) framework. The results indicate that sediments of the Wenliu Member were supplied from four main source areas, including the northwestern Yangchun Uplift, northeastern Enyang low uplift, and southwestern Yangjiang low uplift, with nine major paleochannel clastic sediment transport pathways identified. The different source zones show distinct variations in area, slope characteristics, and sediment supply modes, corresponding to differentiated paleochannel types and paleodrainage configurations. The study area overall exhibits a typical multi-channel convergence depositional pattern, dominated by braid-delta and fan-delta systems. The Enyang low-slope source zone generated the largest braid-delta deposits, whereas fault-transformed source zones produced fan-delta deposits adjacent to active faults and along basin-margin fault systems. Quantitative analysis further indicates that depositional-system scale is significantly correlated with source-area size, paleodrainage development, and paleochannel geometric parameters. Large depositional bodies are more likely to form when the source area exceeds ~60 km^2, the paleochannel width exceeds ~1.4 km, and the cross-sectional area exceeds ~10 km^2. Integrating the spatial relationships among source areas, transport pathways, and depositional systems, four source-to-sink subsystems are identified, which can be further classified into two typical depositional patterns: a long-source gentle-slope braid-delta pattern and a proximal-source rapid-accumulation fan-delta pattern. This study elucidates the coupling relationships among source areas, clastic sediment transport pathways, and depositional sinks in a multi-source rift-lake basin, providing a geological basis for predicting sedimentary systems and guiding hydrocarbon exploration in the study area.

Check for updates

Academic Editor: Manuel Martín-Martín

Received: 30 March 2026
Revised: 21 April 2026
Accepted: 24 April 2026
Published: 29 April 2026

Copyright: © 2026 by the authors. Licensee MDPI, Basel, Switzerland. This article is an open access article distributed under the terms and conditions of the Creative Commons Attribution (CC BY) license.

Keywords: Wenchang Group; Wenliu Member; source-to-sink system; paleochannel; braid delta; fan delta; Yangjiang East Sag

1. Introduction

The source-to-sink (S2S) system refers to the complete process by which surface-derived erosional products are transported from source areas through transport pathways and ultimately deposited in sedimentary basins. It represents a critical subsystem of the deep-time Earth system and reflects the integrated physical, chemical, and biological processes that shape surface material fluxes [1,2]. The launch of the MARGINS Program by the U.S. National Science Foundation in 1998 marked the systematic development of S2S research in sedimentology [3–5]. In recent years, the S2S framework has increasingly become an important tool for linking tectonic evolution, climate change, and sedimentary responses, with its core objective being to reveal the production, transport, and deposition of sediments from source to sink and their dynamic multi-factor coupling [6,7].

Overall, S2S research globally can be summarized in three aspects:

(1) Static elements of S2S systems and provenance identification methods. As the starting point of the S2S system, the nature and distribution of source areas directly control sediment composition and supply intensity. Traditional studies primarily rely on sandstone clast composition, heavy mineral assemblages, and geochemical characteristics for provenance identification [8,9], combined with paleocurrent directions, facies distribution, and well-log data to link sedimentary filling processes with peripheral tectonic evolution [10,11]. In recent years, the widespread application of detrital zircon U–Pb geochronology and Hf isotope tracing has provided high-resolution constraints on the chronological features and tectonic attributes of source areas [12,13]. Furthermore, integrated analyses using geochemistry, clay minerals, and multiple proxies have become mainstream approaches, significantly enhancing the accuracy and reliability of provenance identification [14].

(2) Clastic sediment transport pathways and paleodrainage reconstruction. Transport pathways are the critical links between source and depositional areas; however, their direct preservation in sedimentary records is often limited, making identification and quantitative characterization challenging [6]. Recently, methods for reconstructing paleodrainage systems constrained by paleogeomorphology and three-dimensional seismic data have been developed. By identifying paleochannels, fault-bounded accommodation zones, and structural transfer zones, these approaches allow semi-quantitative characterization of sediment transport paths and transport capacity [15–17]. Studies indicate that channel geometry and spatial arrangement exert significant control on sedimentary body distribution.

(3) S2S coupling processes and quantitative analysis. Coupling within S2S systems represents the current core research focus, aiming to reveal how tectonic activity, climate change, and geomorphic evolution collectively control sediment production, transport, and deposition [7]. Modern sedimentological studies and numerical simulations demonstrate that sediment supply capacity in source areas and transport efficiency in channels jointly determine the scale and spatial patterns of depositional systems [18]. Moreover, the integration of sequence stratigraphy, geological modeling, and process-based sediment simulations has promoted the transition of S2S studies from qualitative analyses to quantitative characterization, gradually establishing multi-scale sedimentary response models [19–21].

In China, significant progress has been made in S2S research on the northern continental margin of the South China Sea, particularly driven by hydrocarbon exploration needs. Studies targeting deep-water depositional systems during the Miocene rifting period have systematically revealed how source-channel-sink coupling controls deep-water sandbody

development [22–24]. Additionally, in the extensive Meso-Cenozoic continental rift basins, prior research on S2S reconstructions has achieved notable advances in methodologies, controlling factors, and coupling patterns [25,26].

However, two key gaps remain in research on source-to-sink systems in continental rift-lacustrine basins. First, most previous studies have focused on single-source or single-depositional systems, and there is still a lack of systematic understanding of how differences among multiple source areas in tectono-geomorphic setting and sediment-supply style influence clastic sediment transport pathways and depositional-system response. Second, under rifting conditions, the relationships among tectono-geomorphic evolution, sediment supply, and basin filling are highly complex, yet the quantitative links among source areas, transport pathways, and depositional systems remain poorly constrained, limiting refined prediction of depositional patterns and favorable reservoirs [27–29].

The Enping 20/21 Depression of the Yangjiang East Sag, Pearl River Mouth Basin, represents a typical rift-lake basin with multi-source supply and complex tectonic settings [30,31]. Previous studies have mainly focused on tectonic evolution and sedimentary system distribution, with a certain understanding of the Paleogene–Neogene Wenchang Group deposition. However, integrated studies of source systems, clastic sediment transport pathways, and depositional systems during the Wenliu Member deposition remain relatively weak. In particular, under multi-source conditions, differences among source areas in supply modes, transport pathways, and depositional system types have not been systematically clarified.

Against this background, this study addresses four research questions: (1) Where were the principal source areas of the Wenliu Member located, and how did they differ in provenance attributes and tectono-geomorphic characteristics? (2) What were the geometric characteristics and spatial organization of the paleochannel transport systems and paleodrainage configurations associated with different source areas? (3) How did different source-area–transport-pathway combinations control the type, scale, and distribution of depositional systems, particularly braided-river deltas and fan deltas? (4) What representative source-to-sink sub-systems and coupling patterns can be identified in this multi-source rift-lacustrine basin? To answer these questions, we integrate drilling, well-log, 3D seismic, heavy-mineral assemblage, and detrital zircon U–Pb age data to systematically identify source areas, characterize clastic sediment transport pathways, and define depositional systems of the Wenliu Member. On this basis, we establish a source-to-sink system framework for the study area and summarize the typical coupling styles in a multi-source rift-lacustrine basin, thereby providing a geological basis for depositional prediction and hydrocarbon exploration.

2. Geological Background

The Pearl River Mouth Basin, located on the northern continental margin of the South China Sea, is a typical Cenozoic rift basin, generally extending in a NE–SW direction. The basin is subdivided into several structural depressions and uplifted blocks. The Yangjiang Depression, situated in the central part of the Zhujiang 3 Depression, is an important sedimentary and hydrocarbon-accumulation area within the basin. The Yangjiang Depression generally trends NE–SW and can be further divided into two subunits, the East Yangjiang Sag and the West Yangjiang Sag. The East Yangjiang Sag consists of multiple secondary subdepressions, including Yangjiang 24 Sag, Enping 19 Sag, Enping 20 Sag, and Enping 21 Sag [23,32]. This study focuses primarily on the Enping 20 Sag and Enping 21 Sag (Figure 1a).

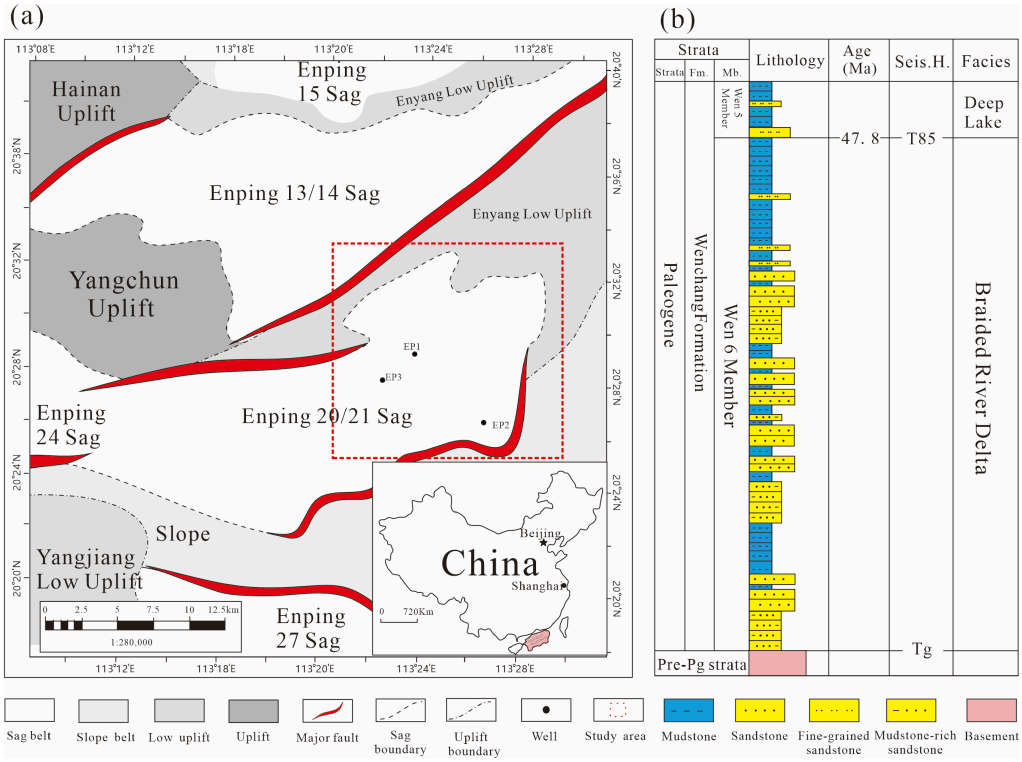


Figure 1. (**a**) Structural map of the East Yangjiang Sag; (**b**) Lithostratigraphic column of the Wenliu Member, Wenchang Group.

The study area is generally controlled by NE–SW trending sag-controlling faults, forming a typical half-graben depression pattern. The F4 and F5 faults are important boundary faults controlling the sedimentary patterns of the Enping 20/21 Sags. These faults not only control the sag morphology and accommodation space distribution but also significantly influence the development of marginal slope belts, sediment supply directions, and the organization of clastic sediment transport pathways [33]. Therefore, although the present study does not focus on tectonic evolution, the current S2S system structure and the spatial distribution of depositional bodies in the study area are still clearly influenced by fault-controlled paleotopography.

The study area preserves a complete Paleogene–Neogene sedimentary sequence, primarily comprising the Wenchang Group, Enping Group, and Zhuhai Group. Among them, the Wenchang Group is the main lacustrine sedimentary unit in the study area and can be further subdivided into multiple depositional members. The Wenliu Member (WSQ1), located in the lower part of the Wenchang Group, is the focus of this study. According to regional stratigraphic division and drilling data, the Wenliu Member was deposited during the rifting stage of the basin, characterized by significant lake-basin subsidence and considerable relief along the basin margins. Sediment from source areas was transported into the lake basin through multiple clastic sediment transport pathways, forming different types of depositional bodies along the basin margin and gentle-slope belts (Figure 1b).

From a sedimentary perspective, the Wenliu Member records a well-constrained linkage between source areas, sediment transport pathways, and depositional systems. On one hand, sediment supply from different directional source areas collectively controls the supply pattern of clastic deposits in the study area. On the other hand, basin-margin slope belts, paleochannels, and local depocenters jointly determine the transport pathways into the lake basin and the depositional style in the sink area. Therefore, the Wenliu Member is an ideal stratigraphic unit for analyzing S2S system architecture.

Magmatic intrusions and tectonic uplifts locally modified stratal thickness and paleotopography through uplift, deformation, and erosion. Post-depositional uplift and erosion have modified the residual stratal thickness and may have altered paleochannel morphology and depositional body boundaries. Therefore, in analyzing the S2S system of the Wenliu Member, erosion-restoration results must be integrated to reconstruct the original basin paleotopography, aiming to restore the depositional-period paleogeographic background and S2S configuration as accurately as possible.

3. Data and Methods

This study integrates core and well-log data from three wells, three-dimensional (3D) seismic data, and provenance analysis results including heavy-mineral assemblages and detrital zircon U–Pb age spectra to conduct a comprehensive study of the source-to-sink (S2S) system of the Wenliu Member (WSQ1) of the Wenchang Group in the Enping 20/21 Sags, East Yangjiang Subdepression, Pearl River Mouth Basin. Well and logging data are primarily used for stratigraphic calibration, facies identification, and well-to-seismic correlation. 3D seismic data are applied for sequence-boundary tracking, paleogeographic reconstruction, paleochannel delineation, and planar distribution analysis of depositional systems. Heavy-mineral assemblages and detrital zircon age data are mainly used to identify the nature of source rocks, constrain sediment provenance, and delineate source areas. The main goal of this study is to identify the spatial relationships among source areas, clastic sediment transport pathways, and depositional systems of the Wenliu Member, thereby establishing a "source–transport pathway–sink" S2S system framework for the study area.

Based on these objectives, the study first performed a unified stratigraphic calibration using existing stratigraphic interpretations and regional correlations, identifying the top and bottom boundaries of the Wenliu Member (WSQ1). Residual stratal thickness maps were compiled to provide fundamental constraints for sediment-source direction analysis and depositional-system characterization. Combining existing paleogeographic knowledge and the structural configuration of the study area, the positions of basin-margin highs, slope-break belts, and potential sediment-source directions were systematically evaluated [34].

In the provenance analysis, heavy-mineral assemblages and detrital zircon U–Pb age spectra were integrated to analyze the source-rock lithology, mineralogical differences, and age-matching relationships of sediments from different directions. This allowed delineation of distinct source areas and constrained the origin of each source belt. For depositional-system identification, a combination of well–seismic integration, seismic facies analysis, and attribute responses was used. Root-mean-square (RMS) amplitude attributes were extracted and combined with waveform clustering results to identify seismic facies belts and depositional-body boundaries. Under well constraints, depositional-system types such as braided-river deltas and fan deltas were distinguished [35].

Finally, based on source-area delineation, paleochannel characterization, and depositional-system identification, the spatial relationships among source belts, transport pathways, and depositional systems were systematically analyzed. This enabled the establishment of S2S subsystems within the Wenliu Member and further summarized the coupling patterns of the source–pathway–sink system in the study area.

4. Results

4.1. Characteristics of Source Areas

Based on paleogeographic restoration and topographic reconstruction of the prototype basin, and integrating multiple provenance tracers such as heavy-mineral assemblages and detrital zircon U–Pb age spectra, the source areas of the Wenliu Member (WSQ1) of the

Wenchang Group in the study area were systematically identified. The results indicate that four major source belts developed in the study area, namely: (I) fault-controlled steep-slope source belt, (II) Enyang gentle-slope source belt, (III) fault-reworked source belt, and (IV) Yangjiang gentle-slope source belt.

4.1.1. Heavy-Mineral Assemblages

Heavy-mineral assemblages, due to their high chemical stability and strong source-rock indication, are important indicators for distinguishing provenance differences [34–37]. Analysis of heavy minerals in the Wenliu Member reveals distinct assemblage types among different source directions and belts. Overall, three main assemblage types can be identified:

Zircon + Titanite + Hematite + Tourmaline + Rutile

Zircon + Titanite + Hematite + Magnetite + Tourmaline + Chlorite

Zircon + Titanite + Hematite + Tourmaline + Hornblende

Among these, the Enyang gentle-slope (II) and fault-reworked (III) source belts are dominated by the "Zircon + Titanite + Hematite + Magnetite + Tourmaline + Chlorite" assemblage, consistent with the heavy-mineral characteristics of the granitic and low-grade metamorphic rocks of the northeastern Enyang low uplift, indicating that sediments in these belts mainly derive from the Enyang low uplift. The fault-controlled steep-slope belt (I) is characterized by "Zircon + Titanite + Hematite + Tourmaline + Hornblende," clearly differing from Enyang low uplift samples; combined with its spatial position, the provenance is interpreted as mafic-intermediate igneous rocks and minor metamorphic rocks of the northwestern Yangchun uplift. The Yangjiang gentle-slope belt (IV) is dominated by "Zircon + Titanite + Hematite + Tourmaline + Rutile," suggesting a source from high-grade metamorphic rocks and felsic gneisses of the Yangjiang low uplift (Figure 2).

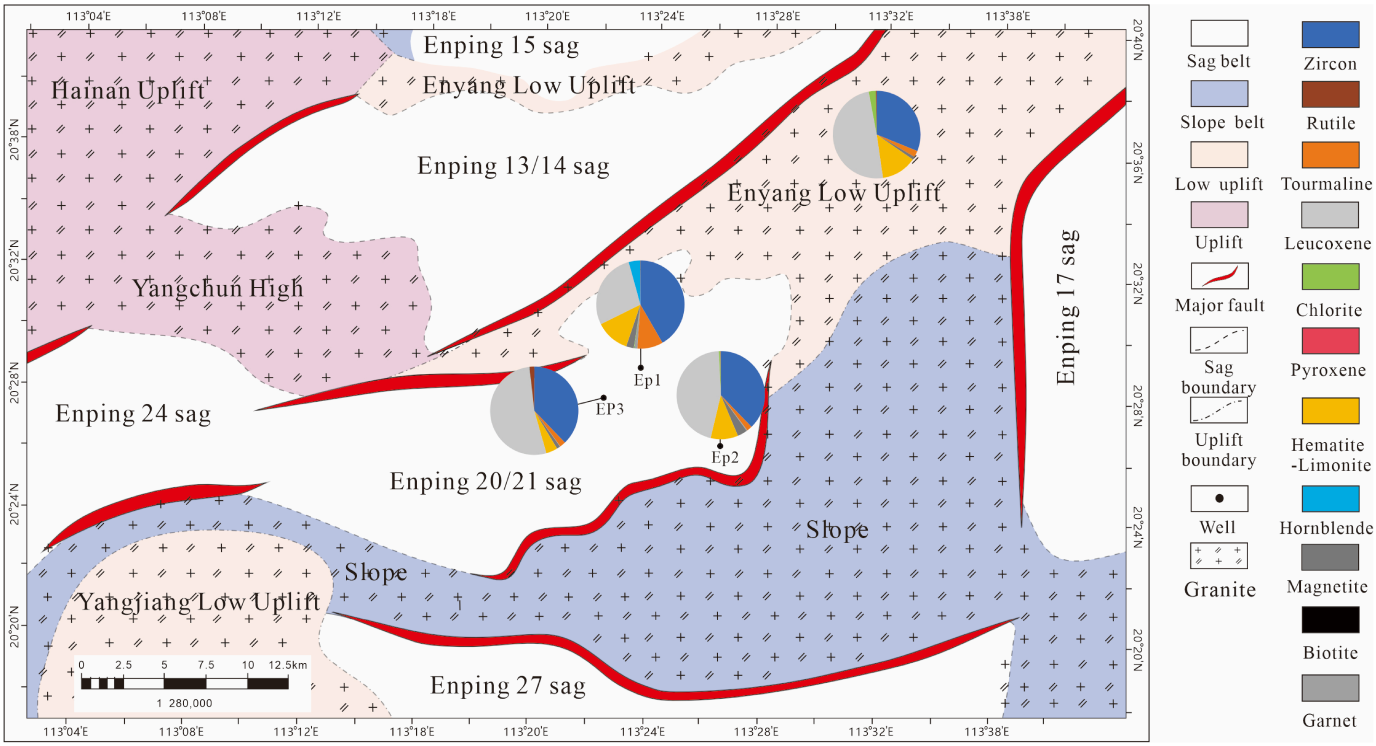


Figure 2. Distribution of Heavy Mineral Assemblages in the Wenchang Formation.

4.1.2. Zircon Age Characteristics

Detrital zircon U–Pb age spectra can accurately reflect the age of source rocks and their material contribution, serving as an important tool for constraining source areas [38–40]. Samples from the Wenliu Member show concentrated age peaks, primarily distributed

between 153–157 Ma, corresponding to magmatic activity in the Late–Middle Jurassic. These ages match the granitic and dioritic intrusions of the surrounding Yanshanian magmatic basement, indicating that the sediments were predominantly derived from erosion of local granitic and intermediate igneous rocks (Figure 3). The consistency between zircon ages and heavy-mineral assemblages provides constraints on both the provenance and the lithology of the source areas.

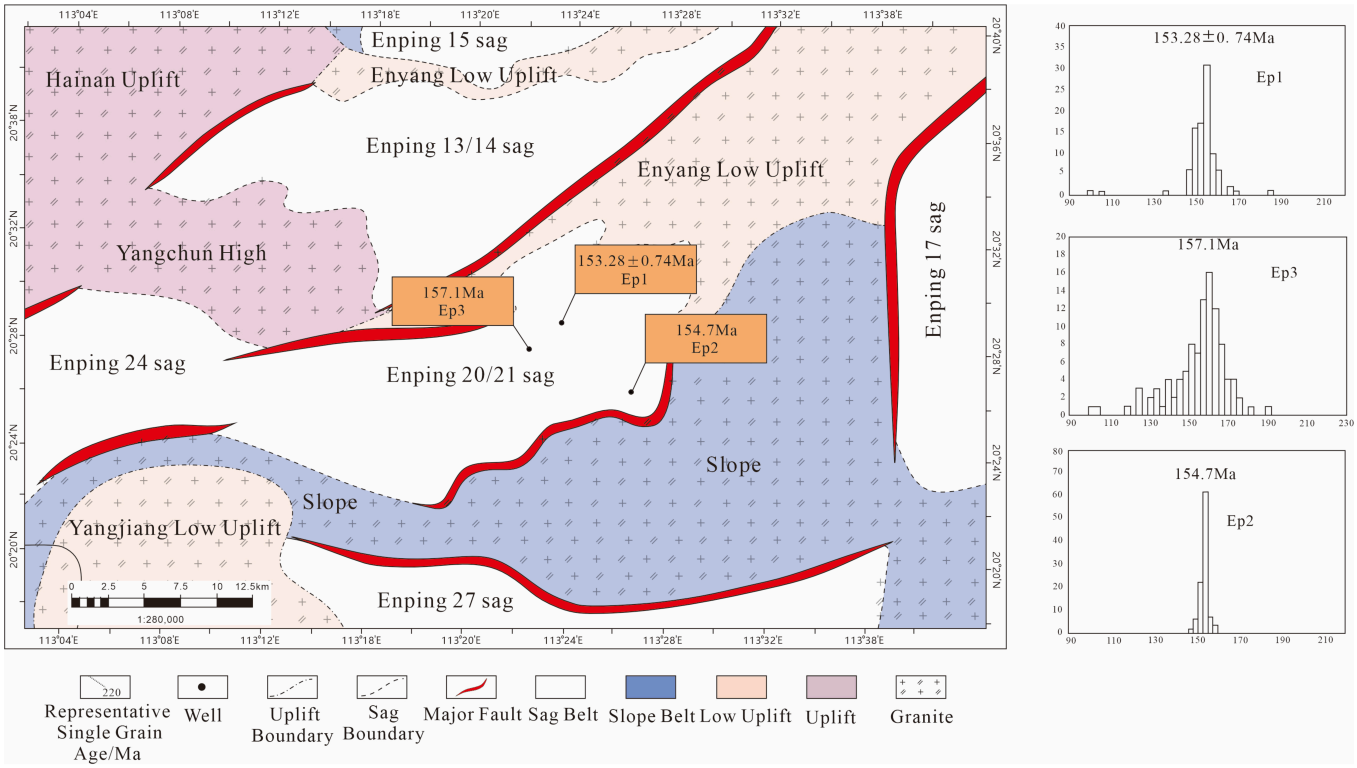


Figure 3. Basement Lithology of the Yangjiang East Depression.

4.1.3. Delineation of Source Belts

Considering the multi-directional sediment supply and the distinct provenance characteristics of the Wenliu Member, source belts were delineated based on heavy-mineral assemblages, detrital zircon age spectra, paleogeographic restoration, and fault structural patterns. By identifying basin-margin highlands, slope-break belt locations, and fault distributions, paleodrainage divides were determined. Using the base of the Wenliu Member as a reference surface and constraining watershed positions with topographic and seismic section morphology (section locations shown in Figure 4a), four major source belts were delineated (Figure 4).

The delineation indicates a clear multi-directional sediment supply pattern:

The fault-controlled steep-slope belt (I) is located in the northwest, sourced from the Yangchun uplift, strongly controlled by the F4 fault, exhibiting typical steep-slope topography with significant relief.

The Enyang gentle-slope (II) and fault-reworked (III) belts are mainly in the northeast, sourced from the Enyang low uplift. The II belt experienced weak structural modification, showing broad, gentle slopes, whereas the III belt was strongly affected by the F5 fault, with a fragmented basement and enhanced topographic relief, displaying clear fault-reworked characteristics.

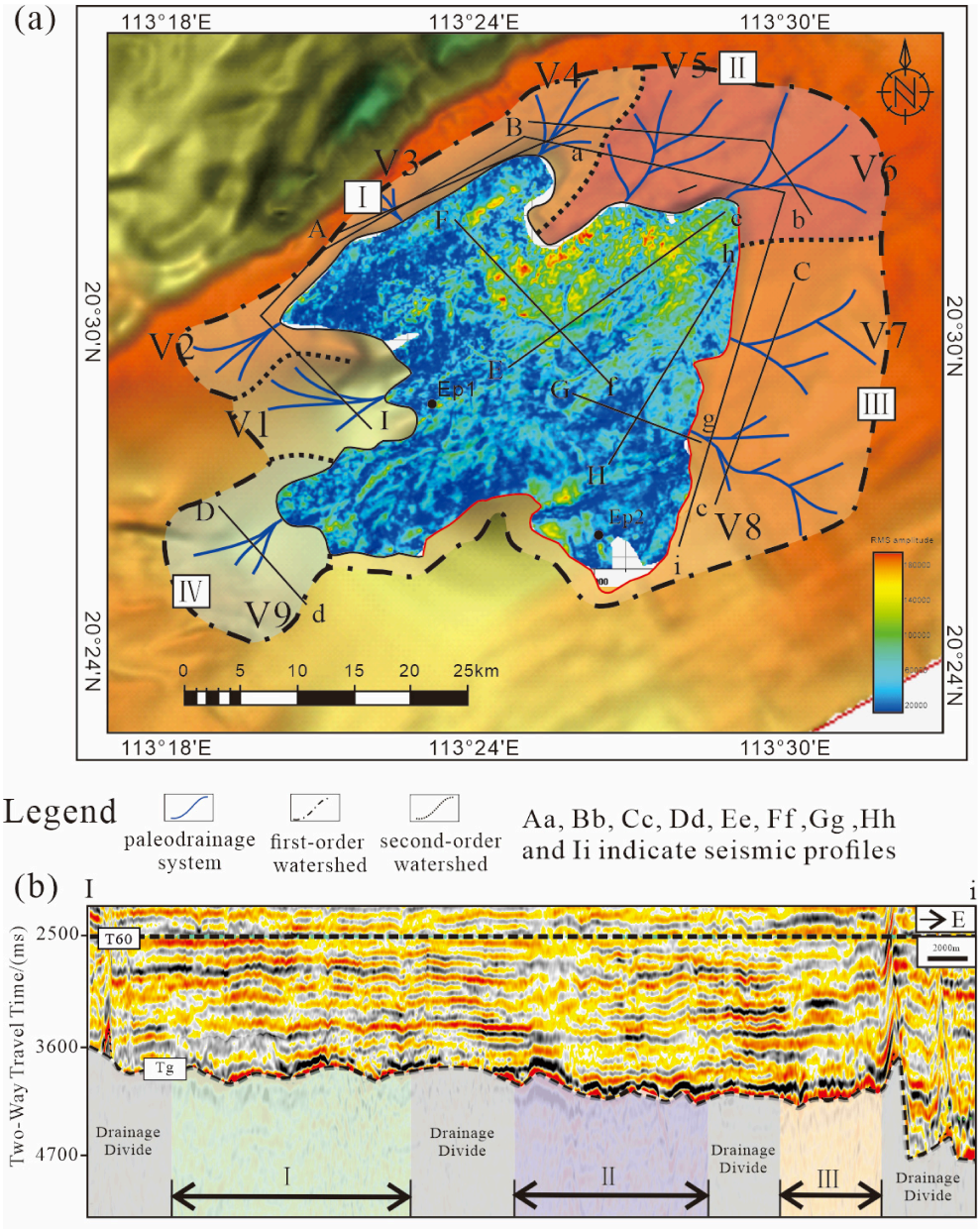


Figure 4. (**a**) Paleogeography, Sediment Source Areas (I: Fault-controlled steep-slope belt; II: Enyang gentle-slope belt; III: Fault-reworked belt; IV: Yangjiang gentle-slope belt), (**b**) Paleodrainage System of the Wenliu Member in the Yangjiang East Depression.

The Yangjiang gentle-slope belt (IV) is in the southwest, sourced from the Yangjiang low uplift, weakly affected by tectonics, generally flat with gentle slopes, representing a typical gentle-slope source area.

Overall, the spatial distribution of source belts is jointly controlled by the northwestern Yangchun uplift, northeastern Enyang low uplift, and southwestern Yangjiang low uplift, overprinted by differential influences of the F4 and F5 faults, forming a well-partitioned multi-source supply pattern that provides material and topographic constraints for subsequent depositional-system development.

4.2. Paleochannel Types and Distribution Characteristics

4.2.1. Characteristics of Paleochannels

Paleochannels were identified based on the reconstructed paleotopography of the prototype basin, seismic cross-section structures, and residual stratigraphic thickness

variations [41–43]. Paleogeographic restoration indicates that during the deposition of the Wenliu Member, the study area exhibited a gradual slope from basin margin to basin center, with multiple source areas forming distinct erosional channels along the slope.

Under 3D seismic constraints, nine major paleochannels (V1–V9) were identified, exhibiting radial and belt-like distributions that correspond spatially to different source areas (Figure 4). Based on cross-sectional morphology and geometric parameters, paleochannels were classified as U-shaped, V-shaped, or W-shaped, reflecting differences in erosion processes and sediment transport dynamics. Source Belt I is dominated by V- and U-shaped channels, indicating strong incision and short-distance sediment transport; Source Belts II and IV mainly develop wide, gentle U-shaped channels with stable, long-distance transport; Source Belt III is dominated by V- and W-shaped channels along fault zones, reflecting strong structural control (Figure 5).

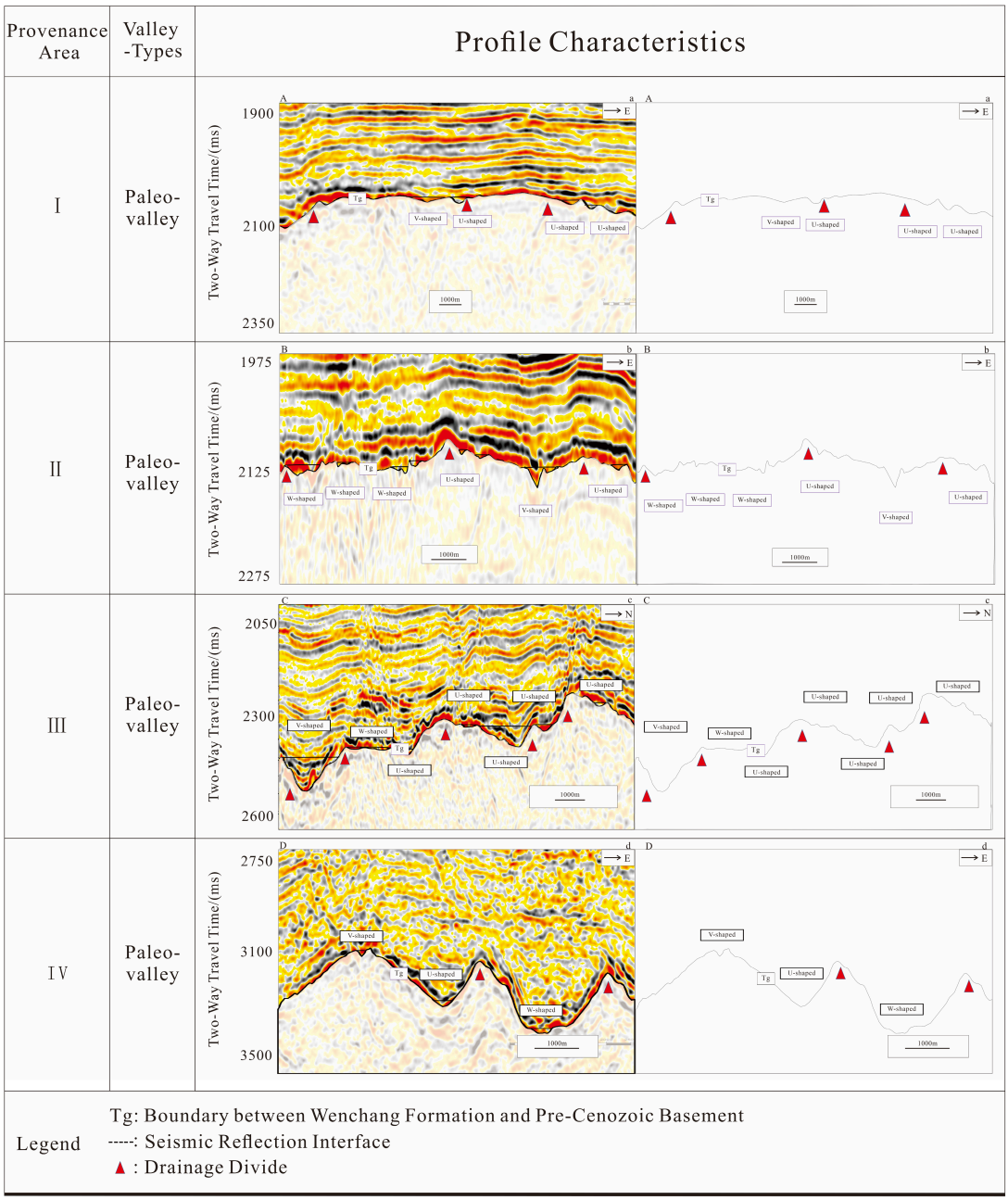


Figure 5. Channel types of paleochannels from different source belts. Cross-section locations are indicated in Figure 4a.

4.2.2. Paleodrainage System Combinations and Distribution Patterns

Analysis of the paleodrainage system shows distinct differences among source belts. Source Belt I develops four small paleochannels (V1–V4) with short transport distances, forming multiple short-branch channels delivering sediment rapidly to the basin margin. Source Belt II contains two main channels (V5–V6), with V5 showing multiple dendritic branches, forming parallel multi-channel drainage; this belt has the highest sediment transport capacity. Source Belt III develops two main channels (V7–V8) along low-lying fault-controlled zones, forming belt-like transport corridors. Source Belt IV only has one main channel (V9) along a gentle slope, providing continuous sediment delivery into the basin (Figure 4).

4.2.3. Paleochannel Geometric Parameters

Geometric parameters of paleochannels (width, depth, width-to-depth ratio) were statistically analyzed to quantify the sediment supply capacity of different source belts (Table 1).

Table 1. Geometric parameters of paleochannels for different source belts in the Wenliu Member.

Source Belt	Channel ID	Width (m)	Depth (m)	Width/Depth Ratio	Main Type
I	V1–V4	64–1250	4.9–42.9 ± 5	8.7–45.5	V-, U-shaped
II	V5–V6	51–1961	9.8–128 ± 15	6.1–36.3	U-, Composite
III	V7–V8	203–1472	7.8–152.7 ± 20	9.6–76.6	V-, W-shaped
IV	V9	1044–1559	82–115 ± 10	11–15	U-shaped

Note: Original depths were in two-way travel time (TWT, ms) and converted to depth (m) using a representative P-wave velocity of 2200 m/s (±300 m/s). Standard deviations reflect uncertainty due to velocity variation and seismic picking.

Channels with large widths or high W/D ratios (e.g., Source Belts II and III) may represent combined statistics of different channel types, and the largest channel depths (~150 m) may correspond to composite channel belts or local incised-valley accumulations rather than single simple channels. Considering potential variations in slope gradient, sediment grain size, and discharge, these geometric parameters are interpreted as relative indicators of sediment transport capacity, rather than absolute measures.

4.3. Sedimentary System Characteristics

4.3.1. Basis for Sedimentary System Identification and Type Characteristics

The identification of sedimentary systems mainly relies on a combination of well-log and seismic analyses, integrating lithological characteristics, seismic reflection structures, and seismic attribute responses to comprehensively determine sedimentary types [44–46]. By combining well-log data, seismic reflection structures, and seismic attribute analyses, two major sedimentary system types are identified in the Wenliu Member (WSQ1) of the study area: braided river deltas and fan deltas, which exhibit distinct depositional features.

The braided river delta system primarily develops in gentle-slope source areas and regions away from basin-margin fault scarps. This system is dominated by medium- to coarse-grained sandstones, interbedded with thin siltstone and mudstone layers. Sedimentary structures mainly include cross-bedding and massive bedding. Well logs display box-like or serrated-box patterns, reflecting high-energy hydrodynamic conditions. On seismic profiles, braided river deltas are characterized by distinct foreset reflection structures, with wedge-shaped bodies prograding toward the basin; internal reflections are relatively continuous (Figure 6). RMS amplitude attributes often show strip-like or patchy high-amplitude anomalies, corresponding to areas of thick sand development (Figure 7a).

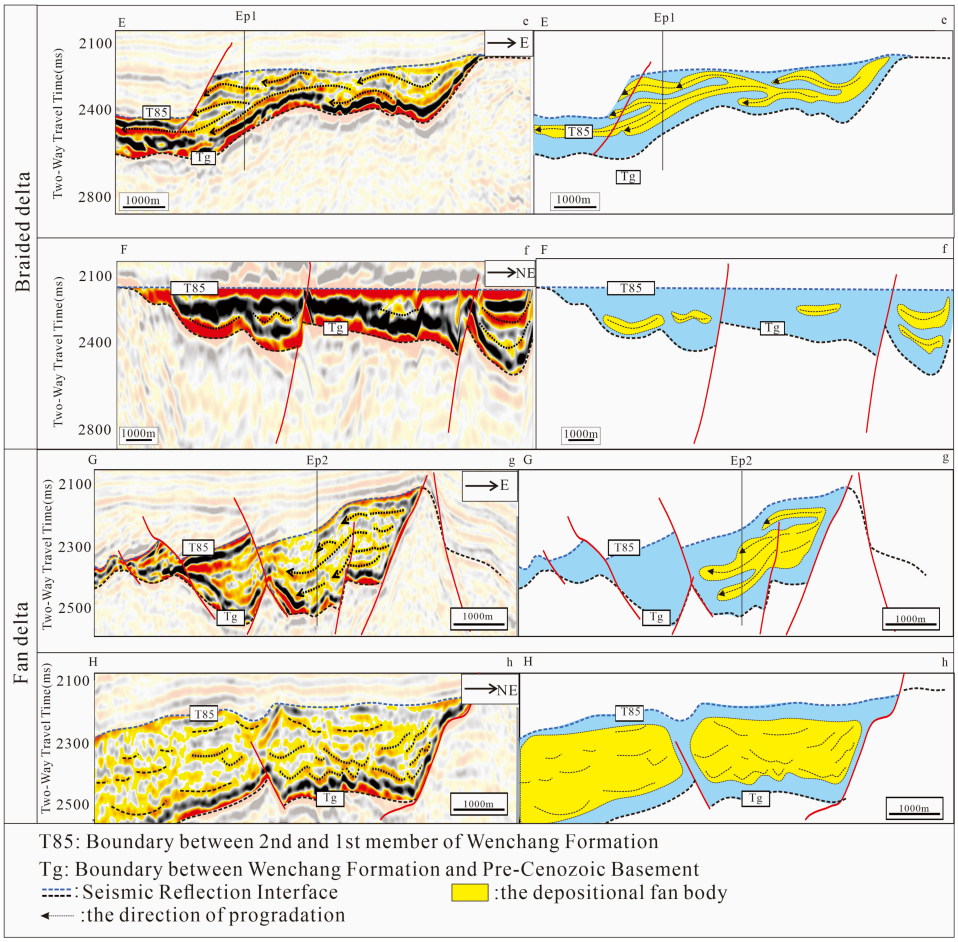


Figure 6. Sedimentary system profile characteristics (profile locations shown in Figure 4a).

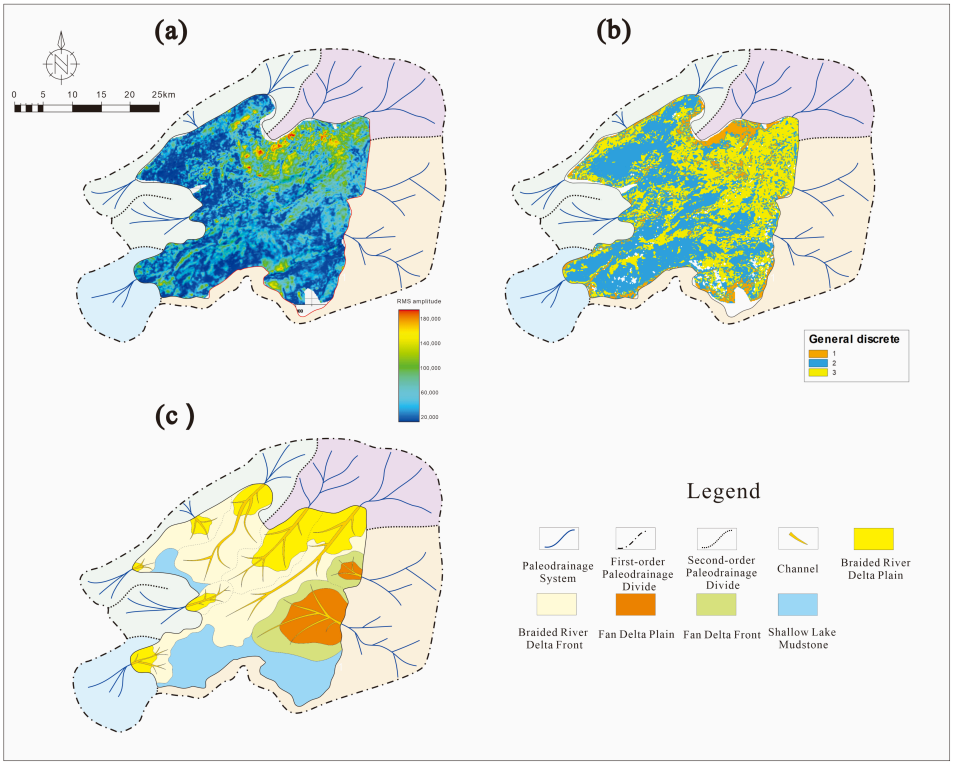


Figure 7. (**a**) RMS attributes of the Wenliu Member; (**b**) waveform clustering; (**c**) sedimentary facies map.

The fan delta system develops near basin-margin fault scarps or fault-controlled source areas. This system contains coarser deposits, commonly coarse sandstones or conglomeratic sandstones, with bedding dominated by massive structures and scour surfaces. Well logs show thick-box or serrated-box features, indicating rapid sediment accumulation. On seismic profiles, fan delta deposits exhibit lens-shaped or wedge-shaped reflection structures with relatively chaotic internal reflections, reflecting rapid deposition and strong gravity-driven transport (Figure 6). RMS amplitude attributes typically present as near-source, high-amplitude, blocky anomalies (Figure 7a).

4.3.2. Depositional System and Scale

Combining the sedimentary system identification results with RMS amplitude attributes and waveform clustering analysis allows characterization of the planar distribution of sedimentary systems in the Wenliu Member (Figure 7c). RMS amplitude attributes primarily identify sand body development zones and the extent of high-energy deposits (Figure 7a), while waveform clustering helps delineate different seismic facies zones, constraining sedimentary system types and their spatial distribution (Figure 7b). Overall, sedimentary systems derived from different source areas exhibit notable differences in scale and distribution.

Source Area I mainly developed a braided river delta system, with a sediment body area of approximately 13 km^2. Sediments are transported rapidly into the basin via short-distance channels, forming near-source fan deposits. Source Area II hosts the largest sedimentary system, with sediment body areas of approximately 48 km^2. Sediments are transported into the basin along multiple channels, forming extensive deltaic deposits. Source Area III, controlled by fault zones, mainly developed linear fan delta systems, with sediment body areas of about 20 km^2 along fault-controlled troughs. Source Area IV exhibits relatively small-scale sedimentary systems, developing minor braided river delta deposits with areas around 14 km^2, extending basinward along gentle slopes.

4.4. Source-to-Sink System Division

Within the framework of source-to-sink analysis, the spatial correspondence between source areas, sediment transport channels, and sedimentary systems is a key criterion for defining source-to-sink sub-systems [47,48]. Based on the previous delineation of source areas, characteristics of paleochannels, and sedimentary system identification, and considering their planar and profile correspondences, four source-to-sink sub-systems are recognized in the Wenliu Member: Fault-Controlled Steep-Slope Sub-system

This sub-system develops along the northern fault scarp zone, with source areas controlled by faults and slope breaks, covering approximately 34.09 km^2. Topography is highly undulating, and sediment supply is dominated by near-source rapid input. Sediment transport channels are mainly V- and U-shaped valleys, forming short-distance, multi-branch networks, allowing rapid sediment delivery into the basin. Corresponding sedimentary systems are braided river deltas, with small sediment body areas of around 13 km^2, primarily near the basin edge.

Enyang Gentle-Slope Sub-system:

Located in the northwest gentle-slope area, the source area covers approximately 66.23 km^2, representing a major sediment supply unit. The wide, gentle topography favors the formation of multiple transport channels, dominated by broad U-shaped valleys and parallel-channel paleodrainage systems. Sediments are continuously transported into the basin, developing the largest braided river delta systems, with sediment body areas of about 48 km^2, indicating extensive distal sand body development.

Fault-Modified Sub-system:

Mainly distributed near central fault zones, covering about 89.42 km^2. Transport channels are dominated by V- and W-shaped valleys along faults, forming linear patterns reflecting strong structural control. Sediments enter the basin along fault-controlled lowlands, forming fan delta systems along structural trends, with sediment body areas around 20 km^2.

Yangjiang Gentle-Slope Sub-system:

Located in the southern gentle-slope area, the source area covers approximately 37.43 km^2. Topography is relatively flat, with stable but limited sediment supply. This sub-system mainly develops broad U-shaped valleys, with few channels and relatively simple transport paths. Corresponding sedimentary systems are small braided river deltas, with sediment body areas around 14 km^2, extending basinward along gentle slopes.

Overall, the source-to-sink structure of the Wenliu Member exhibits clear zonation. Sub-systems differ in source area size, channel arrangements, and sedimentary system types. The fault-controlled steep-slope sub-system shows near-source, short-distance transport; the Enyang gentle-slope sub-system features multi-channel, long-distance transport; the fault-modified sub-system exhibits strong structural control with linear deposits; and the Yangjiang gentle-slope sub-system shows stable but small-scale sediment supply along gentle slopes. Identification of these sub-systems provides a foundation for subsequent source-to-sink coupling analysis and sedimentary pattern interpretation.

5. Discussion

5.1. Sedimentary System Scale Controlled by Source Area and Sediment Transport Path Parameters

To further analyze the relationship between source–sink system architecture and the scale of sedimentary systems, the source area size, paleochannel geometrical parameters, and sedimentary body scale in the study area were statistically analyzed. The results indicate trends linking source-area size, paleochannel geometry, and depositional-body scale (Figure 8).

Statistical analysis shows a general positive relationship between source-area size and the development of the paleodrainage system. Larger source areas typically develop more transport channels, which facilitates sediment delivery, and source-area size is positively associated with depositional-system scale. When source areas exceed approximately 60 km^2, depositional bodies are generally larger than 20 km^2, indicating that adequate sediment supply is a fundamental condition for the formation of large-scale depositional bodies.

Regarding sediment transport paths, paleochannel geometry exerts a key influence on depositional-system scale. Channel width, cross-sectional area, and multi-branch channel networks show positive trends with depositional-body scale. When channel width exceeds ~1.4 km, cross-sectional area exceeds ~10 km^2, and multiple channel branches are developed, sediment can be transported more efficiently into the basin, favoring the formation of larger depositional bodies (Figure 8). This observation aligns with fluvial dynamics principles: wider channels can accommodate higher discharge and enhance particle transport capacity [49].

Channel depth and width-to-depth ratio primarily reflect erosion capacity and have a limited effect on localized transport efficiency, exerting relatively minor control on overall depositional-body scale. Channel length exhibits a negative trend with depositional-body scale, possibly because longer transport paths allow sediment dispersal during transport, while shorter paths facilitate rapid sediment entry and thicker deposition. Given the limited sample size (n = 4 sub-systems), these relationships should be considered preliminary trends rather than absolute quantitative rules.

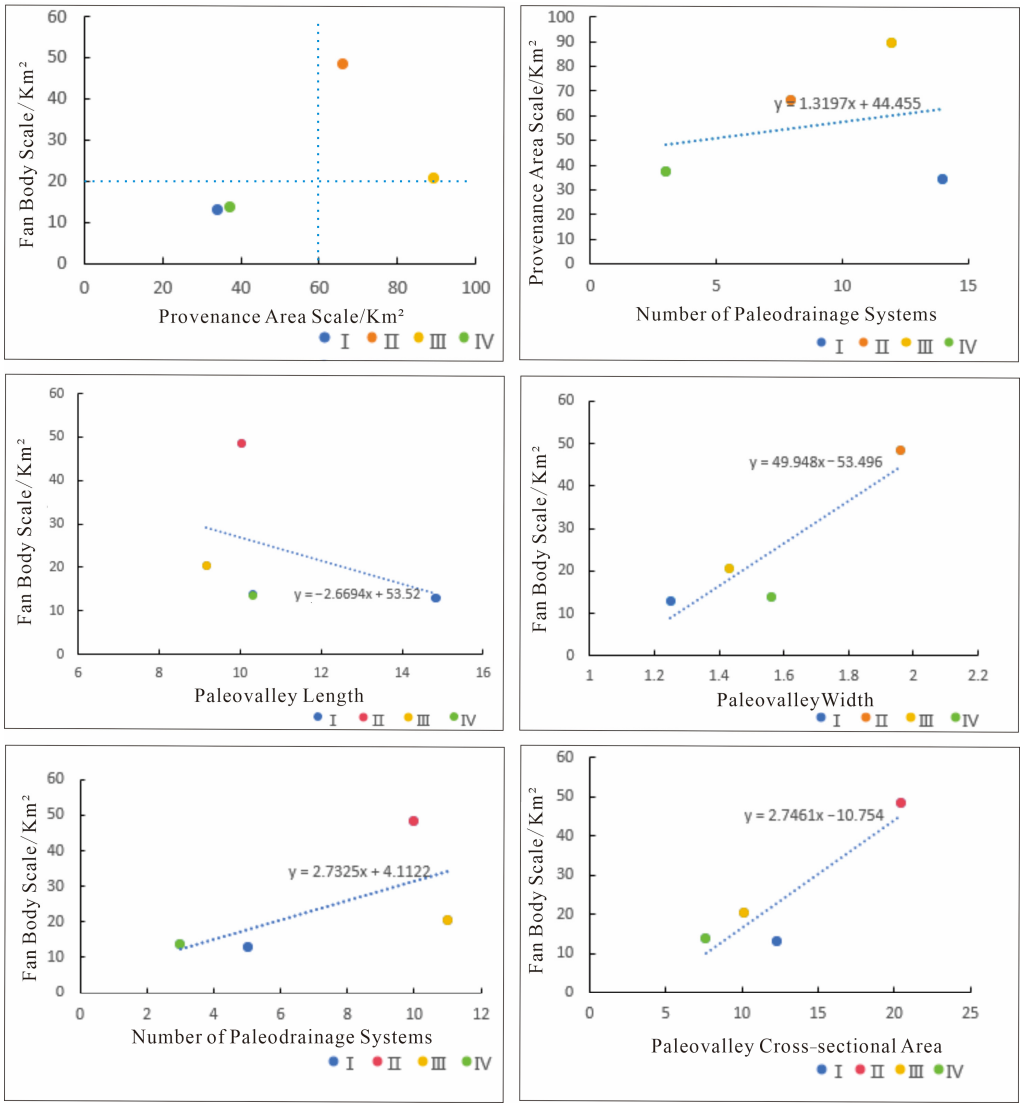


Figure 8. Relationships between fan area, source area, and paleochannel parameters.

Overall, depositional-system scale in the study area is jointly controlled by sediment supply from source areas and transport-pathway structure. Regions with larger source areas and well-developed channels tend to form larger-scale depositional systems, whereas areas with smaller sources or less-developed channels correspond to smaller depositional bodies. In summary, depositional-system scale is influenced not only by source-area size but also by paleochannel geometry and network development, providing quantitative support for understanding source-to-sink coupling.

5.2. Wenliu Formation Source–Sink System Patterns

Integrating source area characteristics, sediment transport path morphology, and sedimentary system distribution, four source–sink subsystems can be identified in the Wenliu Formation of the study area: the fault-controlled steep slope, Enyang gentle slope, fault-modified, and Yangjiang gentle slope subsystems. However, from the perspective of source–channel–sediment body coupling mechanisms, these can be further grouped into two typical sedimentary patterns.

The first pattern is the proximal rapid-deposition fan-delta model (Figure 9a). This model corresponds mainly to the fault-controlled steep slope and fault-modified subsystems. The source area is controlled by steep slopes or faults, with relatively high gradients, and sediment transport occurs mainly through short V-shaped channels or fault-trough

channels. Sediments rapidly enter the basin along steep slopes or structural lows, forming relatively small but thick fan-delta sediment bodies in the sink area. Overall, this pattern is characterized by proximal location, high-energy conditions, and rapid deposition.

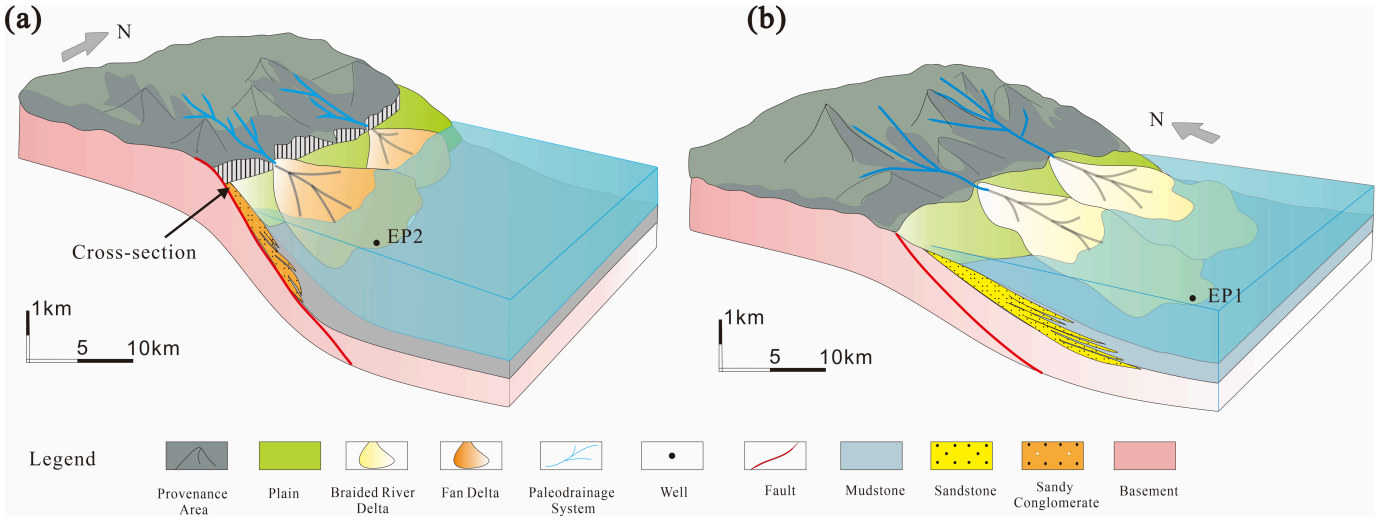


Figure 9. (**a**) Proximal Fan-Delta Depositional Model of the Wenliu Formation Source–Sink System, Yangjiang Depression. (**b**) Distal Braid River Delta Depositional Model of the Wenliu Formation Source–Sink System, Yangjiang Depression.

The second pattern is the distal gentle-slope braid river delta model (Figure 9b). This model mainly corresponds to the Enyang gentle slope and Yangjiang gentle slope subsystems. Source areas are larger with relatively gentle topography, featuring multiple broad and gentle sediment transport channels. The paleo-drainage system consists of parallel multi-channel networks or a single main channel. Sediments are transported over longer distances into the interior of the lake basin, forming large-scale, widely distributed braid river delta systems, characterized by distal sources, continuous sediment supply, and multi-channel distribution.

Although these two depositional patterns are not unique to rift-lacustrine basins, the Wenliu Member provides an example in which multiple source areas with different tectono-geomorphic backgrounds are linked to distinct transport-pathway architectures and depositional-system configurations within the same basin. In this sense, the depositional framework of the study area is more appropriately described as a hierarchical organization composed of multiple source-to-sink sub-systems that can be generalized into two end-member patterns, rather than as a single steep-slope fan-delta model or gentle-slope braided-delta model alone. This interpretation helps to place the depositional fill of the Wenliu Member in a more explicit source-to-sink context and may provide a useful reference for depositional comparison and prediction in other multi-source rift-lacustrine basins.

6. Conclusions

Based on 3D seismic, drilling, and logging data, combined with heavy mineral assemblages and detrital zircon age spectra for source analysis, a systematic study of the Wenliu Formation source–sink system in the Enping 20/21 depression of the Yangjiang Depression, Pearl River Mouth Basin, was conducted, yielding the following insights:

Four main source belts can be distinguished in the Wenliu Formation: (I) fault-controlled steep slope, (II) Enyang gentle slope, (III) fault-modified, and (IV) Yangjiang gentle slope. These source belts show significant differences in sediment provenance direction, area, slope, and sediment supply conditions. Specifically, Belt I derives mainly from the northwest Yangchun uplift; Belts II and III mainly from the northeast Enyang low

uplift; Belt IV mainly from the southwest Yangjiang low uplift, indicating multi-directional sediment supply in the study area.

Nine paleochannel sediment transport paths were identified, with distinct channel types and drainage networks corresponding to different source belts. The northern fault-controlled steep slope belt is dominated by V- and U-shaped channels, forming short-distance, multi-branch networks; the Enyang gentle slope belt develops broad, gentle U-shaped channels forming parallel multi-channel networks; the fault-modified belt develops V- and W-shaped channels along fault lines; the Yangjiang gentle slope belt is characterized by continuous U-shaped channels. These diverse channels together constitute a multi-channel sediment transport system.

Under multiple sediment sources and multi-channel transport, the Wenliu Formation exhibits a "multi-channel convergent" depositional pattern, with braid river deltas and fan deltas as the main sedimentary systems. The Enyang gentle slope source belt forms the largest braid river delta, whereas the fault-modified belt forms fan deltas along structural trends, indicating a clear response of sediment type and scale to source–channel configuration.

Quantitative analyses show that depositional-body scale is positively correlated with source-area size, paleochannel width, cross-sectional area, and number of paleodrainage systems, but negatively correlated with paleochannel length. Source areas > ~60 km^2, channel widths > ~1.4 km, and cross-sectional areas > ~10 km^2 favor the formation of larger-scale depositional bodies, reflecting the combined influence of sediment supply and transport efficiency on body scale.

Integrating source area characteristics, channel structure, and sedimentary system distribution, four source–sink subsystems can be identified: fault-controlled steep slope, Enyang gentle slope, fault-modified, and Yangjiang gentle slope. From a coupling mechanism perspective, these can be grouped into two typical depositional patterns: (i) distal gentle-slope braid river delta, characterized by long-distance, sustained sediment supply, and multi-channel distribution controlling large-scale delta formation; (ii) proximal rapid-deposition fan delta, characterized by fault or slope-controlled rapid sediment input forming thick near-source deltas. These insights indicate a clear zonal coupling in the Wenliu Formation source–sink system, with important implications for sedimentary system prediction and hydrocarbon exploration.

Although this study integrates drilling, well-log, 3D seismic, heavy-mineral assemblage, and detrital zircon U–Pb data to systematically characterize source areas, paleochannel transport pathways, and depositional systems in the Wenliu Member and establishes a source–pathway–sink framework, several limitations remain. First, the quantitative analysis of the source-to-sink sub-systems is based on only four sub-systems, so correlation indicators should be considered preliminary and do not provide high statistical significance. Second, the estimation of paleochannel geometries and depositional-body scales is constrained by the resolution of 3D seismic data, well spacing, and logging precision, which may introduce uncertainties in channel or deposit boundaries. Third, detrital zircon ages and heavy-mineral assemblages reflect integrated provenance information over time and space, potentially masking small-scale variations. Finally, the study area represents a single sag within the Yangjiang East Depression of the Pearl River Mouth Basin, and the applicability of these results to other rift-lacustrine basins or different tectonic settings requires further verification.

Author Contributions: Conceptualization, S.Z. and L.S.; methodology, L.S.; software, L.S.; validation, S.Z., L.S., Y.W., G.G. and R.H.; formal analysis, L.S.; investigation, L.S.; resources, L.S.; data curation, L.S.; writing—original draft preparation, L.S.; writing—review and editing, S.Z., L.S., G.G. and

R.H.; visualization, L.S.; supervision, S.Z.; project administration, S.Z.; funding acquisition, X.Q. All authors have read and agreed to the published version of the manuscript.

Funding: The work was supported by the National Natural Science Foundation of China (grant No. 41472098).

Institutional Review Board Statement: Not applicable.

Informed Consent Statement: Not applicable.

Data Availability Statement: All data and materials are available on request from the corresponding author. The data are not publicly available due to ongoing research using a part of the data.

Conflicts of Interest: Xinwei Qiu was employed by the Shenzhen Branch, CNOOC China Limited. The remaining authors declare that the research was conducted in the absence of any commercial or financial relationships that could be construed as a potential conflict of interest.

References

1. Allen, P.A. From landscapes into geological history. *Nature* **2008**, *451*, 274–276. [CrossRef] [PubMed]
2. Romans, B.W.; Castelltort, S.; Covault, J.A.; Fildani, A.; Walsh, J.P. Environmental signal propagation in sedimentary systems across timescales. *Earth-Sci. Rev.* **2016**, *153*, 7–29. [CrossRef]
3. Leithold, E.L.; Blair, N.E.; Wegmann, K.W. Source-to-sink sedimentary systems and global carbon burial: A river runs through it. *Earth-Sci. Rev.* **2016**, *153*, 30–42. [CrossRef]
4. Kuehl, S.A.; Alexander, C.R.; Blair, N.E.; Harris, C.K.; Marsaglia, K.M.; Ogston, A.S.; Orpin, A.R.; Roering, J.J.; Bever, A.J.; Bilderback, E.L.; et al. A source-to-sink perspective of the Waipaoa River margin. *Earth-Sci. Rev.* **2016**, *153*, 301–334. [CrossRef]
5. Warrick, J.A. Eel River margin source-to-sink sediment budgets: Revisited. *Mar. Geol.* **2014**, *351*, 25–37. [CrossRef]
6. Sømme, T.O.; Helland-Hansen, W.; Martinsen, O.J.; Thurmond, J.B. Relationships between morphological and sedimentological parameters in source-to-sink systems: A basis for predicting semi-quantitative characteristics in subsurface systems. *Basin Res.* **2009**, *21*, 361–387. [CrossRef]
7. Walsh, J.P.; Wiberg, P.L.; Aalto, R.; Nittrouer, C.A.; Kuehl, S.A. Source-to-sink research: Economy of the Earth's surface and its strata. *Earth-Sci. Rev.* **2016**, *153*, 1–6. [CrossRef]
8. Changgui, X.; Weicheng, L.; Yong'an, X.; Shui, Y.; Jianchun, C. Palaeo-geomorphology analysis for the Paleogene reservoir prediction in Bohai Sea area. *Pet. Explor. Dev.* **2004**, *31*, 910–913.
9. Deng, H.W.; Wang, H.-L.; Wang, D.-Z. Control of paleogeomorphology on sequence filling characteristics in continental rift basins: A case study from the Lower Tertiary on the western slope of the Bozhong Depression, Bohai Bay Basin, China. *Oil Gas Geol.* **2001**, *22*, 293–296+303.
10. Guo, T. Provenance Analysis of Daning-Jixianhe 8 Member in Ordos Basin. *Open Access Libr. J.* **2023**, *10*, 1–7. [CrossRef]
11. Peng, Y.; Wang, B.; Yu, H.-Y.; Dong, Y.-Y.; Sheng, L.-N.; Yang, L.-N.; Liu, S.-Z.; Wang, S.-Y.; Zhu, C. Sedimentary system evolution and provenance analysis of the Santanghu Basin: A case study of the Middle–Lower Jurassic in the Tiao-Hu–Malang Sag, Xinjiang, NW China. *Acta Sedimentol. Sin.* **2025**, *43*, 2220–2236. (In Chinese) [CrossRef]
12. Li, Z.; Peng, S. Detrital zircon U–Pb chronology, provenance system analysis, and intraplate basin-mountain evolution of the Meso-Cenozoic strata on the southern and northern flanks of the Tianshan, NW China. *Acta Geol. Sin. (Engl. Ed.)* **2013**, *29*, 739–755.
13. Cui, H.; Wang, C.; Su, M.; Lei, Y.; Zeng, L.; Jia, J. Detrital zircons record the provenance and source-to-sink process in the northwestern margin of the South China Sea. *Front. Mar. Sci.* **2024**, *11*, 1427579. [CrossRef]
14. Garzanti, E.; Pastore, G.; Stone, A.; Vainer, S.; Vermeesch, P.; Resentini, A. Provenance of Kalahari Sand: Paleoweathering and recycling in a linked fluvial-aeolian system. *Earth-Sci. Rev.* **2022**, *224*, 103867. [CrossRef]
15. Sun, X.; Hua, X.; Wang, J.; Yao, C.; Zhang, J. Application of space-time coupling of source-sink sand control principle in sedimentary system research: A case study from the eastern Third Section of Qinhuangdao A structure, Bohai Sea. *J. Xi'an Shiyou Univ. (Nat. Sci. Ed.)* **2017**, *32*, 37–43.
16. Hu, H.W.; Li, H.-Y.; Yu, H.-B.; Xiao, S.-G.; Xu, W. Quantitative analysis of source-to-sink system controls on sand-body distribution of the Paleogene in Chengbei Low Uplift and surrounding areas, Bohai Bay Basin. *J. Palaeogeogr. (Chin. Ed.)* **2020**, *22*, 266–277. [CrossRef]
17. Feng, B.; Li, H.; He, Y.-B.; Li, T.; Du, X.-F.; Huang, X.-B.; Zhou, X.-G.; He, R.-W. Quantitative relationships among source-to-sink system parameters in a lacustrine basin—Taking Miaoxibei Area in Bohai Bay Basin, China as an example. *J. Earth Sci. Environ.* **2023**, *45*, 680–695. [CrossRef]

18. Ji, X.; Xu, C.; Li, W.; Wang, Q.; Hu, H. A quantitative coupling degree model for source-to-sink (S2S) system through entropy weight-coupling theory: A case study of the Chengbei Low Uplift area, offshore Bohai Bay Basin, Eastern China. *Front. Earth Sci.* **2025**, *13*, 1511226. [CrossRef]
19. Ding, X.; Salles, T.; Flament, N.; Rey, P. Quantitative stratigraphic analysis in a source-to-sink numerical framework. *Geosci. Model Dev.* **2019**, *12*, 2571–2585. [CrossRef]
20. Xu, C.; Gong, C. Predictive stratigraphy: From sequence stratigraphy to source-to-sink system. *Oil Gas Geol.* **2023**, *44*, 521–538. [CrossRef]
21. Shafie, K.R.K.; Madon, M. A review of stratigraphic simulation techniques and their applications in sequence stratigraphy and basin analysis. *Bull. Geol. Soc. Malays.* **2008**, *54*, 81–89. [CrossRef]
22. Ren, J.; Xiong, P.; Yu, P.; Peng, Y.U.; Lei, C. Characteristics and formation mechanism of deepwater and ultra-deepwater basins in the northern continental margin of the South China Sea. *Chin. J. Geophys.* **2018**, *61*, 4901–4920. [CrossRef]
23. Liu, Z.; Suo, Y.; Du, X.; Cai, G.; Cheng, H.; Wang, G.; Zhou, J.; Diao, Y.; Fu, X.; Li, S. Site selection for scientific drilling on the continental shelf of the northern South China Sea margin: Implications from sedimentary sources and sinks in the Pearl River Estuary Basin. *Acta Geol. Sin. (Engl. Ed.)* **2022**, *96*, 2775–2787. [CrossRef]
24. Liu, D.L.; Li, H.B.; Wang, P.; Pan, J.W.; Zheng, Y.; Zhu, X.Z. Cenozoic provenance of the northern South China Sea basins and its response to the evolution of surrounding major rivers. *Acta Geol. Sin. (Chin. Ed.)* **2022**, *96*, 2761–2774. [CrossRef]
25. Nie, Y.L.; Zhu, X.; Dong, Y.L.; Yang, K.; Qin, Y.; Ye, L. Characterization and research prospect of source-to-sink system elements in continental rift basin. *Geol. Rev.* **2022**, *68*, 1881–1896. [CrossRef]
26. Zhu, H.T.; Xu, C.G.; Zhu, X.M.; Zeng, H.L.; Jiang, Z.X.; Liu, K.Y. Advances in the coupling research of source-to-sink system elements in continental basins. *Earth Sci.* **2017**, *42*, 1851–1870. [CrossRef]
27. Yu, J.; Liu, T.; Jia, H.; Jiang, Z.; Wei, S.; Li, Y.; Ma, S. Controlling Factors Analyses of Sediment Dispersal From Source-to-Sink Systems of Lacustrine Rift Basin: A Case Study From Paleogene Shahejie-Dongying Formations of Nanpu Sag, Eastern China. *Front. Earth Sci.* **2021**, *9*, 716176. [CrossRef]
28. Teixeira, B.M.N.; Astini, R.A.; Gomez, F.J.; Morales, N.; Pimentel, M.M. Source-to-sink analysis of continental rift sedimentation: Triassic Cuyo basin, Precordillera Argentina. *Sediment. Geol.* **2018**, *376*, 164–184. [CrossRef]
29. Liu, L.; Liu, Z.; Zhao, R.; Cong, L.; Liu, X.; Xin, S.; Mu, Z. The source-to-sink system in continental rift lacustrine basins of the Nantun Formation in X Sag of the Tamtsag Basin, Mongolia. *Sci. Rep.* **2025**, *15*, 25354. [CrossRef]
30. Liu, E.; Chen, S.; Yan, D.; Deng, Y.; Wang, H.; Jing, Z.; Pan, S. Detrital zircon geochronology and heavy mineral composition constraints on provenance evolution in the western Pearl River Mouth basin, northern south China sea: A source to sink approach. *Mar. Pet. Geol.* **2022**, *145*, 105884. [CrossRef]
31. Zhong, L.; Li, G.; Yan, W.; Xia, B.; Feng, Y.; Miao, L.; Zhao, J. Using zircon U–Pb ages to constrain the provenance and transport of heavy minerals within the northwestern shelf of the South China Sea. *J. Asian Earth Sci.* **2017**, *134*, 176–190. [CrossRef]
32. Ge, J.; Zhu, X.; Yu, F.; Jones, B.G.; Tao, W. Controls of faulting on synrift infill patterns in the Eocene PY4 Sag, Pearl River Mouth Basin, South China Sea. *Aust. J. Earth Sci.* **2019**, *66*, 111–132. [CrossRef]
33. Guo, W.; Peng, G.; Chen, Z.; Zheng, X.; Wu, J.; He, J. The role of pre-existing faults in the early–middle eocene palaeogeographic evolution of the PY4 sag, Pearl River Mouth basin, South China Sea. *Mar. Pet. Geol.* **2024**, *165*, 106906. [CrossRef]
34. Morton, A.C.; Hallsworth, C.R. Processes controlling the composition of heavy mineral assemblages in sandstones. *Sediment. Geol.* **1999**, *124*, 3–29. [CrossRef]
35. Brown, A.R. *Interpretation of Three-Dimensional Seismic Data*; American Association of Petroleum Geologists: Tulsa, OK, USA, 2011. [CrossRef]
36. Hubert, J.F. A zircon-tourmaline-rutile maturity index and the interdependence of the composition of heavy mineral assemblages with the gross composition and texture of sandstones. *J. Sediment. Res.* **1962**, *32*, 440–450. [CrossRef]
37. Zhao, L.; Li, Y.; Zou, C.; Zhao, S.; Wu, C. Palaeoweathering Conditions, Provenance, and Tectonic Setting of the Early Silurian Longmaxi Formation in the Upper Yangtze Region (Southern China): Evidence from Geochemistry. *Minerals* **2023**, *13*, 576. [CrossRef]
38. Dickinson, W.R.; Gehrels, G.E. Use of U–Pb ages of detrital zircons to infer maximum depositional ages of strata: A test against a Colorado Plateau Mesozoic database. *Earth Planet. Sci. Lett.* **2009**, *288*, 115–125. [CrossRef]
39. Hadlari, T.; Davis, W.J.; Dewing, K.; Heaman, L.M.; Lemieux, Y.; Ootes, L.; Pratt, B.R.; Pyle, L.J. Two detrital zircon signatures for the Cambrian passive margin of northern Laurentia highlighted by new U-Pb results from northern Canada. *GSA Bull.* **2012**, *124*, 1155–1168. [CrossRef]
40. Wissink, G.K.; Wilkinson, B.H.; Hoke, G.D. Pairwise sample comparisons and multidimensional scaling of detrital zircon ages with examples from the North American platform, basin, and passive margin settings. *Lithosphere* **2018**, *10*, 478–491. [CrossRef]
41. Hampson, G.J.; Storms, J.E.A. Geomorphological and sequence stratigraphic variability in wave-dominated, shoreface-shelf parasequences. *Sedimentology* **2003**, *50*, 667–701. [CrossRef]
42. Lin, C.; Zhang, X.; Huang, S. Review of Late Quaternary incised valley systems. *Geol. Rev.* **2022**, *68*, 627–647. [CrossRef]

43. Snedden, J.W.; Johansen, O.K.; Varhaug, P.; Hvidsten, G.E.; Bakken, K. Seismic, Sedimentologic, and Sequence Stratigraphic Criteria for Recognition of Subsurface Incised-Valley Fills: Mesozoic Strata of the Barents Shelf, Norway. In *Shallow Marine and Nonmarine Reservoirs: Sequence Stratigraphy, Reservoir Architecture and Production Characteristics*; Shanley, K.W., Perkins, B.F., Eds.; SEPM Society for Sedimentary Geology: Claremore, OK, USA, 1997; Volume 18.
44. Zahmatkesh, I.; Kadkhodaie, A.; Soleimani, B.; Azarpour, M. Integration of well log-derived facies and 3D seismic attributes for seismic facies mapping: A case study from mansuri oil field, SW Iran. *J. Pet. Sci. Eng.* **2021**, *202*, 108563. [CrossRef]
45. Torrado, L.; Carvajal-Arenas, L.C.; Mann, P.; Bhattacharya, J. Integrated seismic and well-log analysis for the exploration of stratigraphic traps in the Carbonera Formation, Llanos foreland basin of Colombia. *J. S. Am. Earth Sci.* **2020**, *104*, 102607. [CrossRef]
46. Zhang, J.; Li, S.; Yuan, S.; Long, L.; Yao, J.; Wang, J. Mapping Gravity Flow Depositional Systems using Seismic Sedimentology. *Acta Sedimentol. Sinca* **2015**, *33*, 578–586. [CrossRef]
47. Caracciolo, L. Sediment generation and sediment routing systems from a quantitative provenance analysis perspective: Review, application and future development. *Earth-Sci. Rev.* **2020**, *209*, 103226. [CrossRef]
48. Cao, Y.; Xu, Q.; Wang, J. Progress in research on "source-to-sink" systems in sedimentary basins. *Geosci. Front.* **2018**, *25*, 116–131.
49. Parker, G. Self-formed straight rivers with equilibrium banks and mobile bed. Part 2. The gravel river. *J. Fluid Mech.* **1978**, *89*, 127–146. [CrossRef]

Disclaimer/Publisher's Note: The statements, opinions and data contained in all publications are solely those of the individual author(s) and contributor(s) and not of MDPI and/or the editor(s). MDPI and/or the editor(s) disclaim responsibility for any injury to people or property resulting from any ideas, methods, instructions or products referred to in the content.